Quantum-dot helium: An artificial atom with stunning nonlinear properties

Gilbert Reinisch

Quantum-Dot Helium: an Artificial Atom with Stunning Nonlinear Properties

Gilbert Reinisch*

Université de la Côte d'Azur - Observatoire de la Côte d'Azur
06304 Nice Cedex - France

Abstract

This paper is about a "*number* [which] *has been a mystery ever since it was discovered more than fifty years ago, and all good theoretical physicists put this number up on their wall and worry about it.*" [R. P. Feynman, *QED: The strange theory of light and matter*, Princeton 1985]. This number —Sommerfeld's fine-structure constant $\alpha = e^2/\hbar c \sim 1/137$ — appears quite unexpectedly in the nonlinear mean-field Schrödinger-Poisson (SP) description of a non-relativistic quantum system; namely, quantum-dot helium constituted by a pair of 2D parabolically-confined opposite-spin electrons entangled in the same singlet state. We show by iteration provided by a quickly convergent series of SP nonlinear eigenstates that the non-orthogonality (or inner product) of the two lowest "s" orbitals approaches asymptotically, within less than 0.5% error, the QED (quantum-electrodynamics) electronic amplitude $e^{i\pi}\sqrt{\alpha}$ for photon emission or absorption. The appearance of α in the non-relativistic SP system is explained by the role of virtual photons generated by the nonlinearity of the system.

PACS numbers: 02.60.Lj 12.20.Ds 73.21.La

*Electronic address: Gilbert.Reinisch@oca.eu

In quantum electrodynamics (QED), the fine-structure constant $\alpha = e^2/\hbar c \sim 1/137$ is used as a small parameter for perturbative corrections in the calculation of field-matter interactions. With the use of Feynman diagrams, the contribution of a given perturbative term to the total probability amplitude is a vertex scaled by $\sqrt{\alpha}$. Therefore, in terms of probabilities, these calculations are typically expressed as a quickly convergent series in terms of powers of α [1]. The pioneering example is the anomaly of the electron magnetic moment that paved the way to QED [2]. Rather amusingly, Schwinger's first-order QED correction $\alpha/2\pi$ can be re-written as the mere ratio of Coulomb classical electrostatic energy of a couple of electrons separated by distance λ to Planck quantum energy of that very photon whose wavelength is λ. In [3], it is suggested that α is the ratio of a new elementary quantum of action —namely, e^2/c as the least possible Coulomb interaction — to $\hbar$. The former in conjunction with the latter provides a fundamental basis for understanding the quantum Hall effect, both integral and fractional. In [4], an empirical non-relativistic connection between the electronic polarizability of atoms and α is proposed. The fine-structure constant becomes the ratio between the effective volume of an atom and the volume of a sphere surrounding this atom such that the cloud of virtual photons induced by the presence of matter has its polarizability equal to the atomic polarizability. The virtual photons surrounding the corresponding atom change locally the field properties [5]. In [6] [7], the 97.7% visual transparency of graphene –a two-dimensional material with carbon atoms in a honeycomb lattice— is determined solely by $\pi\alpha$. The significant 2.3% absorption of incident white light despite the graphene being only one atom layer thick is a consequence of graphene's unique electronic structure [8].

These examples show that the appearance of the fine-structure constant α in non-relativistic quantum-mechanics is not an unlikely phenomenon. Within this framework, this letter points out a peculiar relationship between α and a non-relativistic quantum system where nonlinearity plays the major role [9] [10] [11] [12]. The resulting physics could be dubbed "*nonlinear quantum mechanics*". It may appear as an oxymoron since there is no doubt whatsoever that quantum mechanics *is* linear. So why this provocative expression? Because there is a famous precedent within the framework of a possible dual linear/nonlinear complementarity in wave physics: namely, the hydrodynamic solitary-wave example. Since its discovery [13] and its description half a century later by use of the Korteweg-de Vries strongly nonlinear partial differential equation [14], no one suspected a dual linear/nonlinear nature of the solution until the numerical discovery of the "soliton" phenomenon by Zabusky and Kruskal seventy years later [15] —solitons pass through one another without loosing their identity. Three years later, Lax discovered the theoretical explanation by associating nonlinear evolution equations with linear operators so that the eigenvalues of these latter are integrals of the former [16]. This means that the structural properties building the wave coherence are nonlinear while their spectral properties are linear.

This nonlinear-linear wave complementarity echoes a specific nonlinear property of a stationary and separable quantum system which leads to the demonstration of the Born postulate in terms of classical position probability distributions and to the discovery of a new action quantization rule [17]. Transforming Schrödinger's linear and stationary eigenvalue equation into the strongly nonlinear Ermakov wave equation by use of the Madelung-Bohm theory yields an inhomogeneous phase of the wave function which allows the definition of the discrete spectral eigenvalues in terms of phase quantization [18]. Another striking quantum example concerns the canonical transformation of a spin ½ into a classical nonlinear Hamiltonian dynamical system by use of its geometric —or Berry [19]— phase [20]. Contrary to

common sense, this spin ½ global phase becomes an observable property. It defines the 4π symmetry of spinor wave functions (i.e. the sign reversal of the wave function under a 2π rotation [20]) that has been already predicted by Dirac [21] and experimentally observed in both division-of-amplitude [22][23] and division-of-wave-front [24] neutron interferometry experiments (see also [25]). Moreover, this Hamiltonian canonical transformation allows the physical definition, in terms of very-high-frequency oscillations usually discarded in the rotating-wave approximation, of the energy variance of the system [26] whose standard deviation explains the occurence of experimentally observed quantum Zeno jumps [27] [28] [29] [30]. Therefore, like the soliton case in classical physics, these quantum examples display a mathematical *nonlinear*-vs-*linear* duality that provides a remarkable and exact —i.e. distinct from any semiclassical approximation— new link between classical and quantum physics as well as yielding unexpected observable properties.

There is another type of nonlinear quantum approach that, contrary to the above, does not lead to a strict (i.e. mathematically exact) equivalence with linear quantum mechanics. It concerns many-particle Schrödinger description of an interacting quantum system (e.g. via electron electrostatic interaction like in the present work). Because this latter is numerically untractable, it is made computationally reachable by transforming it into a mean-field single-particle model at the cost of making it nonlinear, but numerically solvable [31]. The Hartree, Hartree-Fock and density-functional Kohn-Sham [32] descriptions are approximative mean-field single-particle nonlinear approximations of the originally linear many-particle interacting quantum system (though respectively more and more accurate with increasing particle numbers). However the way nonlinearity is, so to speak, "erased" in order to recover linearity is a bit subtle. Indeed these descriptions are conventionally solved by an iteration scheme where, in each iteration, the mean-field potential is constructed with information about the charge distribution and/or the wave functions from former iterations. Then the resulting Schrödinger equation is considered *linear* within each iteration step and solved by means of standard methods from linear algebra supplying an orthonormal set of eigenfunctions and corresponding eigenvalues. Therefore the original mean-field nonlinearity is rubbed out by use of a (hopefully converging) infinite series of linear Schrödinger descriptions, each being different and characteristic of the iteration step.

There is a more fundamental way to cope with the intrinsic nonlinearity of the mean-field description. It consists in making use of a series of standard iterations like above, but *explicitely keeping nonlinearity within each iteration of the process*; i.e. making use of nonlinear (thus non-orthogonal) eigenstates and of their corresponding eigenvalues at each step of the iteration series. This is the procedure we will use in the present paper. It yields specific physical effects that are not predicted by a standard mean-field approximation defined by its Euler-Lagrange variational solutions. It has indeed been shown [33] that, due to non-orthogonality (or eigenstate overlap defined by their Hilbertian inner product), the ground state defined by a nonlinear single-particle mean-field description is *not* a pure orbital eigenstate like in standard linear quantum theory, but a *mixed state* allowing a small part of the electrons to populate simultaneously higher nonlinear excited energy levels. Therefore eigenstate non-orthogonality leads to quantum correlations defined as usually by the off-diagonal terms of the corresponding density matrix [29] and thus to interferences. Explicit parameters have been provided for the experimental detection of such an interference effect in the case of a GaAs two-level system [33]. *It is crucial to detect it in order to pave the way for a better understanding of the role of nonlinearity in quantum physics.* The reason why such an interference effect has not been predicted by standard Hartree-Fock linear descriptions

might well be that people took it for granted that the Hermiticity of the Hartree-Fock potential operator $\mathcal{W}_{HF}$ yields a complete set of mutually orthogonal eigenfunctions ϕ_i [34] [35]. This is not strictly true because the eigenvalue equation derived from $\mathcal{W}_{HF} \equiv \mathcal{W}_{HF}(\phi_i)$ and defining the ϕ_i's is actually nonlinear.

Quantum-dots can be viewed as artificially structured atoms in heterojunctions or metal-oxide-semiconductor devices where few electrons are confined to a length comparable to the mesoscopic effective Bohr radius a_B ($a_B \sim 10^{-2}$ μm in the case of GaAs). Though the confinement can *a priori* occur in all three directions, some types of experimentally realized quantum-dots display an extension in the $x-y$ plane which is much larger than in the growth direction z of the underlying semiconductor structure [36–38]. Therefore, these quantum-dots are usually regarded as artificial atoms with a disk-like shape. Since electron numbers as low as one or two per dot have already been realized [36, 38], quantum-dot helium consisting of two electrons trapped in the two-dimensional (2d) axisymmetrical harmonic potential $V(r) = \frac{1}{2}m\omega^2 r^2$, where $r^2 = x^2 + y^2$ and m is the effective electron mass, is actually the simplest realistic model for an interacting quantum system [39, 40]. As itself or amongst other such few-electron systems, it has been extensively studied in the relationship with the development of nanotechnologies [37] [41].

The present paper provides a nonlinear mean-field integro-differential model for a couple of opposite-spin electrons entangled in the same state and harmonically confined in a 2D quantum-dot helium system [40]. We restrict its spectrum to the two lowest "s" states (no angular momentum). This model is the simplest —and probably the most accurate— nonlinear mean-field approximation of the original two-particle interacting linear Schrödinger equation for the seven following reasons:

1. In a *parabolically-confined* electron gas, the center-of-mass and the internal degrees of freedom are completely decoupled, due to the generalized Kohn theorem [42, 43]. Since we are only interested in the internal structure of the two-particle wave function, the parabolic confinement ensures that there will not be any perturbation of this internal state by some external "frozen" center-of-mass degree of freedom.

2. The parabolic confinement is mathematically equivalent to plasma oscillations of an electron gas over a continuum of positive charges uniformly distributed in space ("jelium"). This jelium background provides charge neutrality of the system in its Thomas-Fermi limit [12]. Such a property can be of interest in the investigation of the nature of High-T_c superconductor Cooper pair "glue" [44].

3. The paper considers "s" (zero-angular-momentum) orbital eigenstates in order to discard any parasite spin-orbit coupling. Therefore the eigenstates have *radial symmetry*.

4. The coupling of the Poisson equation with the 2d Schrödinger equation is mathematically consistent only if the fomer is appropriately modified to comply with Gauss' asymptotic electrostatic potential created by the 2d electron gas. The present paper provides this modification by introducing an ad-hoc specific r^{-1} factor in the source term of the Poisson equation.

5. A pair of confined electrons constitutes the simplest and most accurate mean-field model for bounded interacting quantum systems. Due to the use of Koopmans' theorem for the determination of its energy levels [45], one does not need to average over several surrounding electrons in order to define the effective mean-field that yields

the density of charges [46]. The 2nd fellow-electron's potential alone actually *is* this effective mean field.

6. A $S = 0$ *singlet-spin* (or opposite-spin) electron pair allows to consider those eigenstates where the two particles lie *both* in the same "s" orbital state in agreement with the Pauli exclusion principle. So they are *entangled* and constitute a pair of "orbital bosons" defined by the same wavefunction [47]. In this configuration, there is neither exchange energy nor, like already mentioned above, spin-orbit coupling.

7. A *two-state model* is a reasonable choice, due to the absence of spectral dispersion [48]. This choice is also consistent with the Wigner-Weisskopf approximation for the Schrödinger equation in the interaction representation [49].

Consider the 2D radial-symmetrical quantum-dot helium described by its real-valued dimensionless mean-field orbital state $u(X)$ where X is the radius. The two opposite-spin electrons are entangled in the *same* "s" —zero angular momentum— orbital state $u(X)$ [50]. We call m the effective particle mass (possibly taking into account quasiparticle effects) and Ω the angular frequency of the external harmonic trap. In appropriate units where the parabolic confinement becomes $X^2/4$, the corresponding nonlinear integro-differential stationary Schrödinger equation with eigenvalue μ and electron charge e reads:

$$\frac{d^2}{dX^2}u + \frac{1}{X}\frac{d}{dX}u + \Big[\mu - \Phi - \frac{1}{4}X^2\Big]u = 0, \tag{1}$$

where energy is given in units of $\hbar\Omega$ and the electrostatic interaction energy Φ is defined as:

$$\Phi(X) = \int_0^\infty \Big[u(X')\Big]^2 G(X,X')X'dX', \tag{2}$$

by use of its Green function:

$$G(X,X') = \frac{1}{\pi}\int_0^\pi \big[X^2 - 2XX'\cos\phi + X'^2\big]^{-1/2}d\phi. \tag{3}$$

The system of Eqs. (1-3) will be solved by the following iterative procedure where $\Phi^{(n)}$ is a functional of $u^{(n-1)}$:

$$\frac{d^2}{dX^2}u^{(n)} + \frac{1}{X}\frac{d}{dX}u^{(n)} + \Big[\mu^{(n)} - \Phi^{(n)} - \frac{1}{4}X^2\Big]u^{(n)} = 0, \tag{4}$$

$$\Phi^{(n)}(X) = \int_0^\infty \Big[u^{(n-1)}(X')\Big]^2 G(X,X')X'dX'. \tag{5}$$

The initial/boundary conditions that define a regular even "s" eigensolution are:

$$[u^{(n)}(X)]_{X=0} = u_0^{(n)} \quad ; \quad \Big[\frac{d}{dX}u^{(n)}(X)\Big]_{X=0} = 0, \tag{6}$$

and

$$\lim_{X\to\infty} u^{(n)}(X) = 0. \tag{7}$$

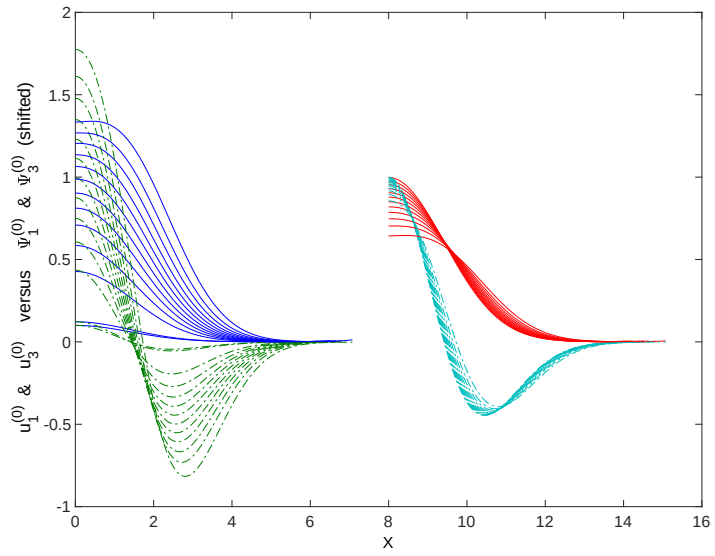

FIG. 1: The two lowest s eigenstates u_1 (continuous blue) and u_3 (dashed green) of the nonlinear differential system (8-13) versus their corresponding actual wavefunctions Ψ_1 and Ψ_3 defined by (15) and normalized to unity. Their common nonlinearity parameter (14) increases from 0.01 to 8 and so do the l.h.s.profiles. To the contrary, the r.h.s. amplitude of $\Psi_{1,3}$ decreases with increasing N.

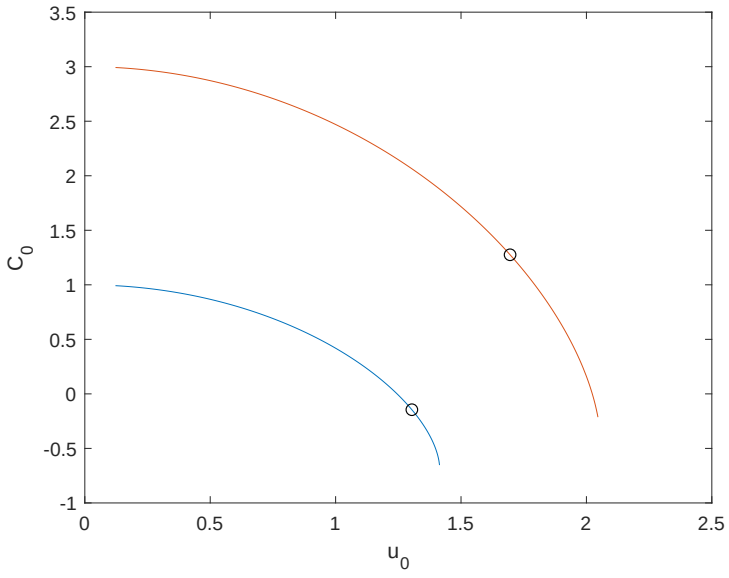

FIG. 2: The respective trajectories of the inital conditions of eigenstates u_1 (lower blue plot) and u_3 (upper red plot) defined by (10-11) when their common nonlinearity parameter N defined by (14) increases from the quasilinear value 0.01 —hence $C_{1,3} \sim \mu_{1,3} \sim 1$, 3 in agreement with (17)— to 8. The circles correspond to the minimum inner product displayed by Fig. 3

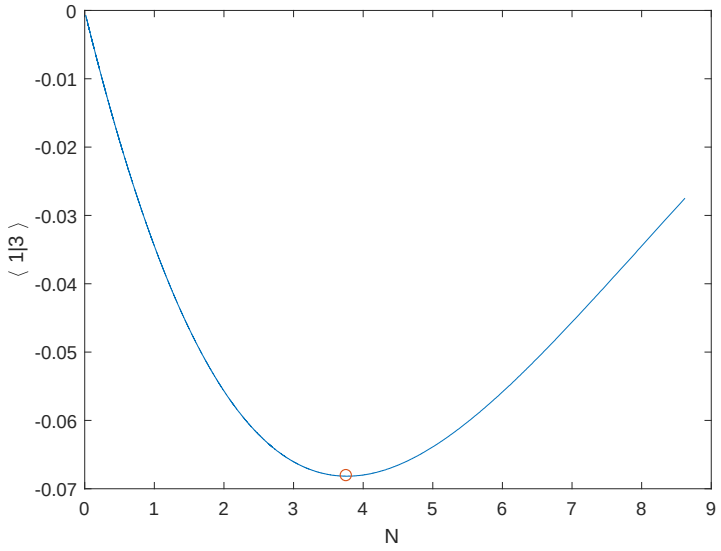

FIG. 3: The inner product (20) corresponding to Fig. 1 when the nonlinearity parameter N —see definition (14)— increases from 0.01 to 8. The circle displays the minimum $\langle u_1|u_3\rangle_{min} = -0.0682$ at $N = 3.747$.

The initial profile $u^{(n-1)}(X) = u^{(0)}(X)$ corresponding to $n = 1$ in Eq. (5) can be defined by any of the discrete eigensolutions u_i of the following Schrödinger-Poisson (SP) nonlinear differential system (we drop superscript $^{(0)}$ for the sake of clarity):

$$\frac{d^2}{dX^2}u_i(X) + \frac{1}{X}\frac{d}{dX}u_i(X) + \left[C_i(X) - \frac{1}{4}X^2\right]u_i(X) = 0, \tag{8}$$

and

$$\frac{d^2}{dX^2}C_i(X) + \frac{2}{X}\frac{d}{dX}C_i(X) = \frac{[u_i(X)]^2}{X}. \tag{9}$$

It is solved by use of the initial conditions at $X = 0$:

$$[u_i(X)]_{X=0} = a_i \quad ; \quad \left[\frac{d}{dX}u_i(X)\right]_{X=0} = 0, \tag{10}$$

$$[C_i(X)]_{X=0} = b_i \quad ; \quad \left[\frac{d}{dX}C_i(X)\right]_{X=0} = \frac{1}{2}{a_i}^2, \tag{11}$$

where a_i and b_i are the two real-number free parameters that define the nonlinear eigensolution $\{u_i(X), C_i(X)\}$ of differential system (8-9). They are chosen in agreement with the two following eigenstate constraints for all discrete nonlinear eigenstates i:
1) Regularity:

$$\lim_{X\to\infty} u_i(X) = 0 \quad \forall i, \tag{12}$$

2) Normalization for all discrete nonlinear eigenstates $u_i(X)$:

$$\int_0^\infty \left[u_i(X)\right]^2 X dX = N \quad \forall i, \tag{13}$$

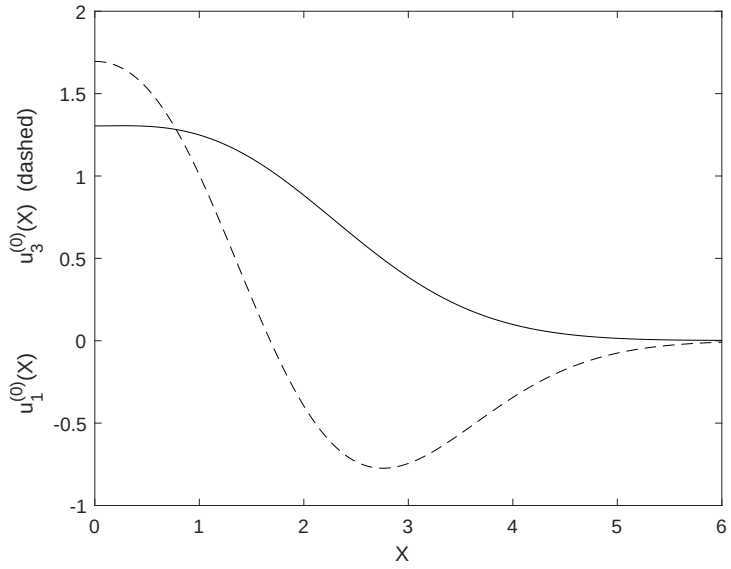

FIG. 4: The two lowest s eigenstates, namely ground state u_1 (continuous) and excited state u_3 (dashed), defined by the nonlinear differential system (8-13) at the minimum of inner product $\langle u_1|u_3\rangle = -0.0682$ when $N = 3.747$ (circle in Fig. 3)

.

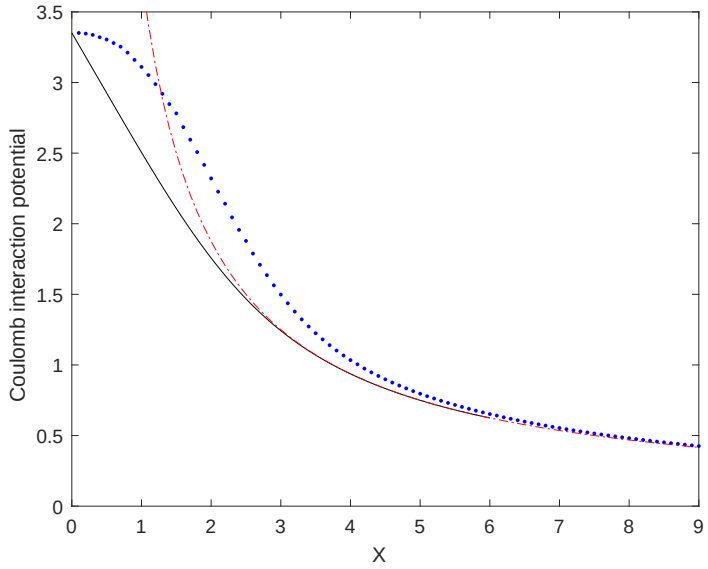

FIG. 5: The ground-state Coulomb interaction $\Phi_1(X)$ (continuous black plot) as the nonlinear solution of Eqs (8-13) and (16-18) at $N = 3.747$ (circle in Fig. 3), compared with the blue dotted next-step Coulomb interactions $\Phi_1^{(1)}(X)$ defined by Eq. (5) for $n = 1$. Both Coulomb interactions do agree with Gauss' asymptotic behaviour $N/X = 3.747/X$ defined by Eq. (19) and displayed by the red point-dashed plot.

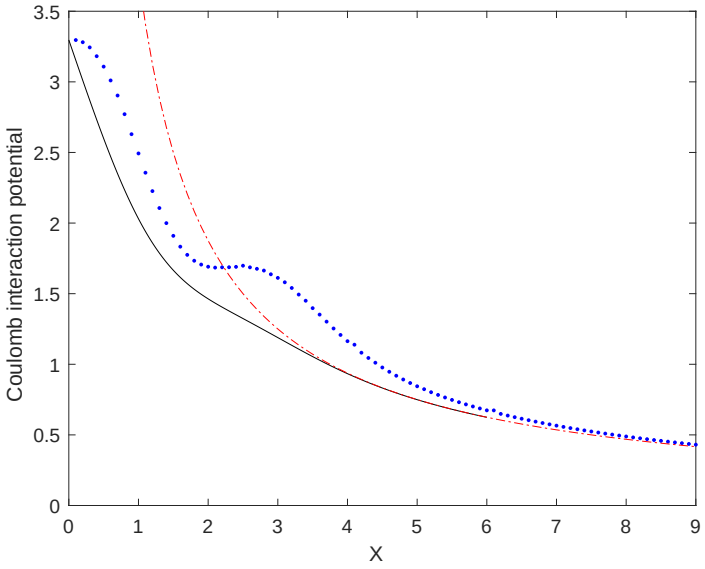

FIG. 6: The same as in Fig. 5 for the excited state $|3\rangle$.

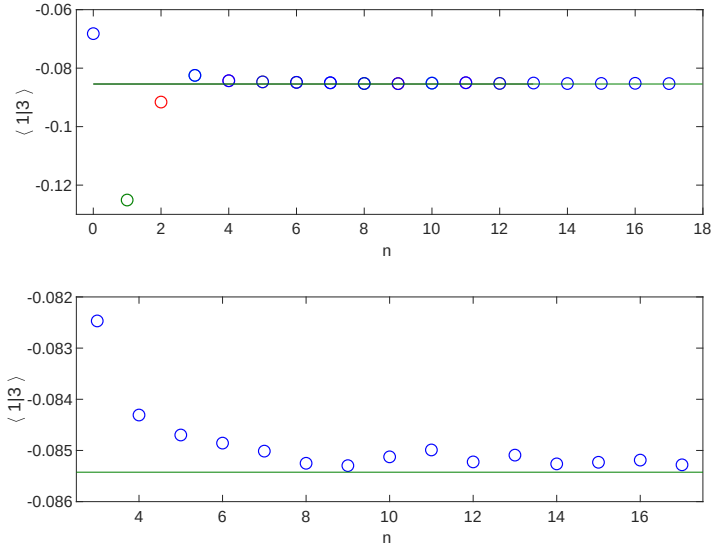

FIG. 7: The inner product (21) obtained about $N = 3.747$ (circle in Fig. 3) by the iteration process (4-7) til $n = 17$ shown at two different vertical scales. The horizontal line displays the QED amplitude $e^{i\pi}\sqrt{\alpha}$ for photon emission or absorption by an electron that is defined by the fine-structure constant $\alpha = 1/137.035999....$

where the dimensionless parameter

$$N = \frac{e^2/L}{\hbar\Omega} \tag{14}$$

is given by the experimental conditions of the quantum dot; namely, the harmonic length $L = \sqrt{\hbar/2m\Omega}$ of its confining parabolic potential $V(r) = \frac{1}{2}m\Omega^2 r^2$ which becomes $\frac{1}{4}X^2$ when

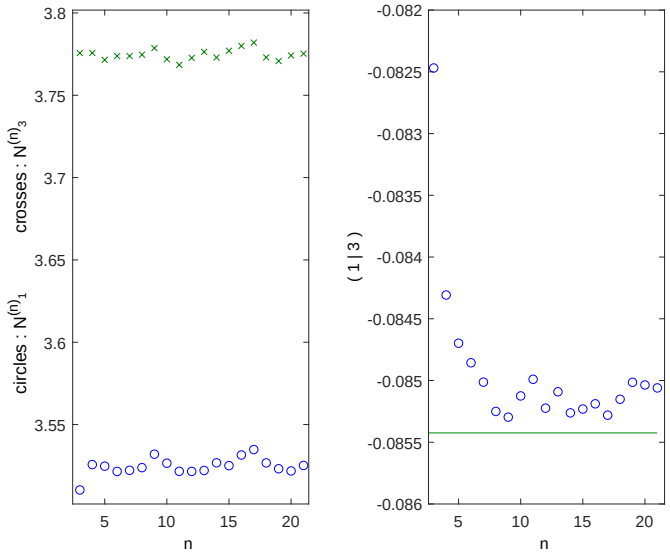

FIG. 8: The respective norms $N_{1,3}^{(n)}$ which define the solution $u_{1,3}^{(n)}$ of Eq. (4) for $n \leq 21$ (left), displayed opposite the corresponding inner product (21).

$X = r/L$ and all energies are given in units of $\hbar\Omega$ (e and m being respectively the charge and the mass of the electron including if necessary quasiparticle effects). Then Eqs (13-14) yield the expected 2D normalization of the electron-pair wavefunction Ψ_i:

$$\Psi_i(r) = \frac{1}{L\sqrt{2\pi N}}\, u_i[X(r)] \quad \rightarrow \quad \int_0^\infty \Psi_i^2(r) 2\pi r dr = 1. \tag{15}$$

Note that N defined by Eq. (14) should be regarded as the nonlinear order parameter of the system since it compares the classical electrostatic energy e^2/L between the two confined electrons with the harmonic quantum gap $\hbar\Omega$ defining the parabolic confinement. Therefore it yields a quantitative description of the quantum-classical transition from the highly quantum regime $e^2/L \sim \hbar\Omega$ when $N \sim 1$ [50] —the quantum dot has a quasilinear behaviour with negligible particle-particle interaction when $N \rightarrow 0$— to the classical case *à la Thomas-Fermi* in the opposite strongly nonlinear case $N \gg 1$ [12].

Once any discrete eigensolution $u_i(X)$ of the nonlinear differential system (8-9) is obtained by the appropriate choice of a_i and b_i in accordance with Eqs (10-13), its corresponding chemical potential (or nonlinear eigenvalue) μ_i is given by:

$$\mu_i = C_i(X) + \Phi_i(X), \tag{16}$$

(cf. Eq. (4)) where $\Phi_i(X)$ is defined as the functional of $[u_i(X)]^2$ by Eq. (2). In particular, at $X = 0$:

$$\mu_i = b_i + \varphi_i, \tag{17}$$

where

$$\varphi_i = \Phi_i(0) = \int_0^\infty \Big[u_i(X')\Big]^2 \frac{1}{X'} X' dX' = \int_0^\infty \Big[u_i(X')\Big]^2 dX' \tag{18}$$

by use of Eq. (2) together with its Green function (3).

The discrete regular eigensolutions $u_i(X)$ of the nonlinear differential system (8-13) are the $n = 1$ zeroth approximation of the iterative solution defined by Eqs (4-7). The present letter considers the two lowest "s" eigenstates u_1 and u_3. They are displayed by Fig. 1, using (as for all numerical results given in the present paper) the MATLAB R 2018b routine (options = odeset('RelTol',1e-10)) for integration. It shows $u_1(X)$ (continuous blue) and $u_3(X)$ (dashed green) when their common nonlinearity parameter N defined by Eq. (14) increases from 0.01 to 8. These normalized eigenstates are labelled in agreement with their respective energies 1 and 3 (in units of $\hbar\Omega$) in the linear limit $N \to 0$: see Fig. 2 which shows the respective trajectories of their inital conditions (10-11) as N varies. These latter go clockwise when N increases and eventually reach their second-order phase transition which describes the wavefunction change from the constant-width piling-up regime to the constant-amplitude spreading-out one [50]).

The X^{-1} factor in the source term of the r.h.s. of Poisson equation (9) is due to Gauss' theorem. Indeed, when $X \to \infty$, the electrostatic interaction Φ defined by Eqs (9) and (16) yields as expected:

$$\lim_{X\to\infty} \Phi(X) = \frac{N}{X}, \tag{19}$$

since N defines the total charge of the 2D reduced electron density in accordance with Eq. (13): see Figs 5-6. In contrast, droping the X^{-1} factor in the r.h.s. of Eq. (9) would yield the 3D electron density integral $\lim_{X\to\infty} \Phi(X) = X^{-1} \int_0^\infty [u(X')]^2 X'^2 dX'$ which is obviously electrostatically incorrect for the 2D electron density u^2: compare with the expected 2D one in (19), namely, $X^{-1} \int_0^\infty [u(X')]^2 X' dX' = N/X$.

The 2D eigenstate non-orthogonality $\langle u_1|u_3\rangle \neq 0$ is given by the following inner product:

$$\mathcal{P}_1 = \langle u_1|u_3\rangle = \frac{1}{\sqrt{N_1 N_3}} \int_0^\infty u_1 u_3 X dX, \tag{20}$$

for the two nonlinear eigenstates $u_{1,3}$ are displayed by Fig. 1. Their common norms $N_1 = N_3 = N$ is defined by Eqs (13-14): see Fig. 3 which shows their (weak) non-orthogonality. At the minimum $\langle u_1|u_3\rangle_{min} = -0.0682$ reached for $N = 3.747$ (circle in Fig. 3), the corresponding eigenstate profiles are displayed by Fig. 4 while their respective Coulomb interactions $\Phi_1(X)$ and $\Phi_3(X)$ defined by Eqs (16-18) are shown by the continuous black plots in Figs 5 and 6. Like emphasized above in (19), these figures also show that both Coulomb interactions do agree with Gauss' asymptotic behaviour $N/X = 3.747/X$ as they should. The next-step Coulomb interactions $\Phi^{(1)}_{1,3}(X)$ are defined by Eq. (5) for $n = 1$ from the zeroth-order eigenstate profiles u_1 and u_3 shown in Fig. 4. They are respectively displayed by the dotted blue plots in Figs 5 and 6. Then the iteration process described by Eqs (4-5) with initial & boundary conditions (6-7) goes on until a quasi-stationary asymptotic regime apparently occurs for the nth (say, $8 \leq n \leq 21$) inner product:

$$\mathcal{P}_n = \langle u_1^{(n)}|u_3^{(n)}\rangle_{8\leq n\leq 21} = e^{i\pi}\sqrt{\alpha} + \epsilon \quad ; \quad \epsilon \sim 5\,10^{-4}. \tag{21}$$

The corresponding values are shown by the blue circles as a function of the iteration rank n in Figs. 7 and 8. The relative error defined by ϵ is $\sim 0.5\%$ with respect to the horizontal line $e^{i\pi}\sqrt{\alpha} = -0.08542...$ that displays in amplitude and phase the QED photon emission or absorption process by an electron [1]. The asymptotic eigenstate overlap (21) illustrated by Figs. 7 and 8 numerically demonstrates that α's numerical value $\sim 1/137$ can indeed be defined with a precision of $\sim 99\%$ about the minimum $\langle 1|3\rangle_{min}$ of eigenstate overlap amplitude

(20) by a mathematical solution solely based on the nonlinear properties of the dimensionless integro-differential system (1-3). Let me stress the profound underlying signification of this result and list the physical arguments that support it.

1. The iteration described by Eqs (4-5) with initial/boundary conditions (6-7) yields eigenstate renormalization at each step n of the process. Indeed the two nth solutions $u_{1,3}^{(n)}$ are each confined in their own potential $\frac{1}{4}X^2+\Phi_{1,3}^{(n)}$ (this latter being respectively defined by $u_{1,3}^{(n-1)}$). Therefore these two potentials are *different* and *change* after each iteration. So will consequently do their respective norms $N_{1,3}^{(n)}$ defined by Eq. (13), yielding $N_1^{(n)}\neq N_3^{(n)}$ for $n\geq 1$ as shown by Fig. 8.

2. The limit displayed by the horizontal line in Figs. 7 and 8 equals $e^{i\pi}\sqrt{\alpha}$ that defines the QED amplitude for photon emission or absorption by an electron [1].

3. This finding is *not* accidental and does *not* belong to numerology. Indeed the two first nonlinear eigenstates of quantum-dot helium interfere, due to the following theorem related to the Hermitian properties of the Laplacian operator [33]:

$$\langle u_1|u_3\rangle=\frac{{\Phi^1}_{13}}{\mu_1-\mu_3}+\frac{{\Phi^3}_{31}}{\mu_3-\mu_1}. \tag{22}$$

   The subscripts in ${\Phi^i}_{jk}$ define the matrix elements of the particle-particle interaction Φ_i corresponding to eigenstate $|u_i\rangle$: see Eq. (16).

4. By extrapolation from first-order time-independent perturbation theory in quantum mechanics [51] (actually related to Fermi's golden rule), the first term in the r.h.s. of Eq. (22) defines an absorption-like transition; namely, the probability amplitude for the system being in the nonlinear ground eigenstate $|u_1\rangle$ to populate the nonlinear excited eigenstate $|u_3\rangle$, due to interaction Φ_1 defined by the probability density $|u_1|^2=u_1^2$, while the second term defines the reverse process induced by interaction Φ_3 defined by u_3^2; namely, the probability amplitude for the system being in the excited eigenstate $|u_3\rangle$ to populate the ground state $|u_1\rangle$ through an emission-like transition. These two $|u_1\rangle\leftrightarrow|u_3\rangle$ emission-absorption amplitudes interfere in the build-up of the inner product $\langle u_1|u_3\rangle$ as shown by Eq. (22).

5. The amplitudes are in phase and add up resonantly at any extremum of the inner product. This occurs at the minimum $N=3.747$ displayed by the circle in Fig. 3. According to QED, this simultaneous resonant emission-absorption process can be performed by a virtual photon mediating in the electrostatic field. It is defined in its Feynman diagram by a first-order amplitude closed loop $\propto\sqrt{\alpha}$ that describes this particular photon-electron interaction [52]. This is precisely that very limit $\propto\sqrt{\alpha}$ which is displayed by the horizontal line in Figs. 7 and 8.

As the conclusion of this letter, let me stress that the present work claims 99% of the solution of "*one of the greatest damn mysteries in physics*" according to Feynman [1]; namely, the numerical value $\sim 1/137$ of the fine-structure constant $\alpha=e^2/\hbar c$. The 1% missing is likely due to the approximative mean-field stationary Hartree description of a parabolically-confined opposite-spin interacting electron pair entangled in the same low-energy orbital

state (quantum-dot helium). Despite this rather severe approximation, the resulting ninety-nine percent conclusion that this numerical value $\sim 1/137$ is of transcendental mathematical origin (say, like π or e) and hence stable is of interest (e.g., in astrophysics [53, 54]).

Specific nonlinear quantum properties have been emphasized in this work. i) Quantum nonlinearity defines eigenstate overlap that leads to QED's virtual photon generation. ii) These photons stimulate in turn transitions between nonlinear eigenstates with probability proportional to α. iii) Comparing these virtual photon transitions with maximum eigenstate overlap yields the 99% accurate numerical value of α.

These pivotal advances might influence the research of others to converge towards the experimental value $\alpha = 7.297...\,10^{-3}$ by using in the present model a more accurate nonlinear mean-field description of, e.g., the density-functional theory type [31, 32], combined with higher-order QED terms [52]. Indeed, the numerical value of α "*has been a mystery ever since it was discovered ... and all good theoretical physicists put this number up on their wall and worry about it.*" [1].

---

[1] R. P. Feynman, *QED: The Strange Theory of Light and Matter*, Chapt. 4 (Princeton, 1986).

[2] J. Schwinger, Phys. Rev. **73**, 416 (1948), https://doi.org/10.1103/PhysRev.73.416.

[3] R. Wadlinger, G. Hunter, L. Kostro, and D. Schuch, Physic Essays **3**, 194 (1990).

[4] A. Tkatchenko, D. V. Fedorov, and M. Gori, J. Phys. Chem. Lett. **12**, 9488 (2021), doi: 10.1021/acs.jpclett.1c02461.

[5] G. Compagno, S. Vivirito, and F. Persico, Phys. Rev. A At., Mol., Opt. Phys. **46**, 7303 (1992).

[6] R. R. Nair, P. Blake, A. N. Grigorenko, K. Novoselov, T. J. Booth, T. Stauber, N. M. Peres, and A. K. Geim, Science **320** (2008), doi: 10.1126/science.1156965.

[7] J. Reed, B. Uchoa, Y. Joe, Y. Gan, D. Casa, E. Fradkin, and P. Abbamonte, Science **330**, 805 (2010), doi: 10.1126/science.1190920.

[8] S.-E. Zhu, S. Yuan, and G. Janssen, Europhysics Letters **108**, 17007 (2014), doi: 10.1209/0295-5075/108/17007.

[9] G. Reinisch, J. of Phys.: Conference Series **237**, 012019 (2010).

[10] G. Reinisch and M. Gazeau, Eur. Phys. J. Plus **131**, 220 (2016), doi 10.1140/epjp/i2016-16220-6.

[11] G. Reinisch, J. Laser Opt. Photonics **5** (2018), int. conf. on quantum mechanics and applications, Atlanta (USA) doi: 10.4172/2469-410X-C3-030.

[12] G. Reinisch, Eur. Phys. J. Plus **134**, 573 (2019), doi.org/10.1140/epjp/i2019-12967-4.

[13] J. Scott Russel, Fourteenth meeting of the British Association for the Advancement of Science (1844).

[14] D. J. Korteweg and G. de Vries, Philosophical Magazine **39**, p. 422–443 (1895).

[15] N. J. Zabusky and M. D. Kruskal, Phys. Rev. Lett **15**, 240 (1965).

[16] P. D. Lax, Comm. on Pure and Applied Math **21**, 4 (1968).

[17] G. Reinisch, Phys. Rev. A **56**, 3409 (1997).

[18] G. Reinisch, Physica A Statistical Mechanics and its Applications **206**, 229 (1994).

[19] J. C. Solem and L. C. Biedenharn, Foundation of Phys. **23**, 185 (1993).

[20] G. Reinisch, Physica D **119**, 239 (1998).

[21] D. Park, *Classical dynamics and its quantum analogues* (Springer, 1990), 2nd ed., ISBN 0-387-51398-1.

[22] H. H. Rauch, A. Zeilinger, G. Badurek, A. Wilting, W. Bauspiess, and U. Bonse, Phys. Lett. A **54**, 425 (1975).
[23] S. Werner, R. Colella, A. Overhauser, and C. Eagen, Phys. Rev. Lett. **35**, 1053 (1975).
[24] A. Klein and G. Opat, Phys. Rev. Lett. **37**, 238 (1976).
[25] M. E. Stoll, E. K. Wolff, and M. Mehring, Phys. Rev. A **17**, 1561 (1978), doi.org/10.1103/PhysRevA.17.1561.
[26] G. Reinisch, arXiv:2205.12763 [quant-ph] (2022), https://doi.org/10.48550/arXiv.2205.12763.
[27] Z. Minev, S. Mundhada, S. Shankar, P. Reinhold, R. Gutiérrez-Jáuregui, R. Schoelkopf, M. Mirrahimi, H. Carmichael, and M. Devoret, Nature **570**, 200 (2019).
[28] G. Reinisch, Results in Physics **29**, 104761 (2021), doi.org/10.1016/j.rinp.2021.104761.
[29] G. Reinisch, Annals of Phys. **449**, 169205 (2023), https://doi.org/10.1016/j.aop.2022.169205.
[30] G. Reinisch, Physica E: Low-dimensional Systems and Nanostructures **154**, 115787 (2023), doi: 10.1016/j.physe.2023.115787 hal-04168845.
[31] W. Kohn, Rev. Mod. Phys. **71**, 1253 (1998).
[32] W. Kohn and L. Sham, Phys. Rev. **140**, A1133 (1965).
[33] G. Reinisch and V. Gudmundsson, Eur. Phys. J. B **84**, 699 (2011), doi: 10.1140/epjb/e2011-20725-5.
[34] E. K. U. Gross, E. Runge, and O. Heinonen, *Many-Particle Theory* (Adam Hilger, 1991).
[35] A. Galindo and P. Pascual, *Quantum Mechanics II* (Springer, 1991).
[36] C. Sikorski and U. Merkt, Phys. Rev. Lett **62**, 2164 (1989).
[37] P. A. Maksym and T. Chakraborty, Phys. Rev. Lett **65**, 108 (1990).
[38] R. C. Ashoori, H. L. Stormer, J. S. Weiner, L. N. Pfeiffer, K. W. Baldwin, and K. W. West, Phys. Rev. Lett. **71**, 613 (1993).
[39] U. Merkt, J. Huser, and M. Wagner, Phys. Rev. B **43**, 7320 (1991).
[40] D. Pfannkuche, V. Gudmundsson, and P. Maksym, Phys. Rev. B **47**, 2244 (1993).
[41] M. Wagner, U. Merkt, and A. Chaplik, PHys. Rev. B **45**, 1951 (1992).
[42] W. Kohn, Phys. Rev. **123**, 1242 (1961).
[43] S. M. Reimann and M. Manninen, Rev. Mod. Phys. **74**, 1283 (2002).
[44] J. Zaanen, *100 years of superconductivity: A modern, but way too short history of the theory of superconductivity at a high temperature*, vol. 2.4 (Chapman and Hall, 2011), arXiv:1012.5461v2.
[45] A. Szabo and N. S. Ostlund, *Modern Quantum Chemistry: Introduction to Advanced Electronic Structure Theory,* (Dover, 1996).
[46] G. Reinisch, J. Pacheco, and P. Valiron, Phys Rev. A **63**, 042505 (2001).
[47] G. Reinisch, Phys. Rev. A **70**, 033613 (2004).
[48] H. Eleuch and I. Rotter, Eur. Phys. J. D (2015), http://dx.doi.org/10.1140/epjd/e2015-60389-7.
[49] W. H. Louisell, *Radiation and Noise in Quantum Electronics* (McGraw-Hill Book Company, 1964).
[50] G. Reinisch and V. Gudmundsson, Physica D **241**, 902 (2012).
[51] L. D. Landau and E. M. Lifshitz, *Quantum Mechanics* (Pergamon Press, London, 1958).
[52] R. D. Mattuck, *A guide to Feynman diagrams in the many-body problem*, ISBN: 0-486-67047-3 (Dover, 1992).
[53] A. Shlyakhter, Nature **264**, 340 (1976).
[54] M. Wilczynska, J. Webb, M. Bainbridge, J. Barrow, S. Bosman, R. Carswell, M. Dąbrowski, and V. Dumont, Science Advances **6** (2020), doi: 10.1126/sciadv.aay9672.

Acknowledgments

The author gratefully acknowledges technical support from UMR *Lagrange* (Observatoire de la Côte d'Azur, université de Nice, France) as well as useful criticism from Guillaume Dujardin (INRIA, Lille, France).

The data that support the findings of this study are available from the corresponding author upon reasonable request.